Original Article

Digestive Diseases

Dig Dis 2014;32:658–663
DOI: 10.1159/000367982

Genome-Wide Profiling of DNA Methylation and Tumor Progression in Human Hepatocellular Carcinoma

Naoshi Nishida[a, c] Takafumi Nishimura[d] Takuya Nakai[b] Hirokazu Chishina[a] Tadaaki Arizumi[a] Masahiro Takita[a] Satoshi Kitai[a] Norihisa Yada[a] Satoru Hagiwara[a] Tatsuo Inoue[a] Yasunori Minami[a] Kazuomi Ueshima[a] Toshiharu Sakurai[a] Masatoshi Kudo[a]

Departments of [a]Gastroenterology and Hepatology and [b]Surgery, Kinki University Faculty of Medicine, Osaka-Sayama, and [c]Department of Gastroenterology and Hepatology, Kyoto University Graduate School of Medicine, and [d]Outpatient Oncology Unit, Kyoto University Hospital, Kyoto, Japan

Key Words
CpG sites · Cytosine residues · DNA methylation · Genome-wide profiling · Hypomethylation

Abstract
Objective: To clarify the progression pattern of abnormal DNA methylation during the development of hepatocellular carcinoma (HCC) using a comprehensive methylation assay. ***Methods:*** We used an Infinium HumanMethylation450 BeadChip array that can analyze >485,000 CpG sites distributed throughout the genome for a comprehensive methylation study of 117 liver tissues consisting of 59 HCC and 58 noncancerous livers. Altered DNA methylation patterns during tumor progression were also analyzed. ***Results:*** We identified 38,330 CpG sites with significant differences in methylation levels between HCCs and noncancerous livers (DM-CpGs) using strict criteria. Of the DM-CpGs, 92% were hypomethylated and only 3,051 CpGs (8%) were hypermethylated in HCC. The DM-CpGs were more prevalent within intergenic regions with isolated CpGs. In contrast, DM-CpGs that were hypermethylated in HCC were predominantly located within promoter regions and CpG islands ($p < 0.0001$). The association between methylation profiles of DM-CpGs and tumor size was statistically significant, especially in hepatitis C virus (HCV)-positive cases ($p = 0.0001$). ***Conclusions:*** We clarified the unique characteristics of DM-CpGs in human HCCs. The stepwise progression of alterations in DNA methylation was a common feature of HCV-related hepatocarcinogenesis.

Introduction

Hepatocellular carcinoma (HCC) is a common malignancy worldwide, and the at-risk population is still growing [1, 2]. Several reports have suggested that hepatocarcinogenesis involves multiple molecular pathways with the accumulation of genetic and epigenetic alterations, including point mutations and abnormal DNA methylation [3–6].

Methylation of cytosine residues at cytosine-guanine dinucleotides (CpG sites) is commonly found in eukary-

KARGER

E-Mail karger@karger.com
www.karger.com/ddi

0257–2753/14/0326–0658$39.50/0

Naoshi Nishida, MD
Department of Gastroenterology and Hepatology
Kinki University Faculty of Medicine
337-2 Ohno-Higashi, Osaka-Sayama, Osaka 589-8511 (Japan)
E-Mail naoshi@med.kindai.ac.jp

otic DNA, including human DNA, and carries important epigenetic information required for proper gene function [7]. For example, DNA methylation contributes to the regulation of gene transcription as well as the stabilization of chromosomes [8]. It is well known that the pattern of DNA methylation found in normal cells is handed down to the daughter cells during mature cell division. However, alterations in the DNA methylation profile of mature cells are frequently observed in many types of human cancers, including HCC [9]. The regional hypermethylation of a gene promoter is typically associated with transcriptional inactivation of corresponding tumor suppressor genes, while global hypomethylation can induce genomic instability, a process that can play an important role in carcinogenesis [3]. Therefore, it is necessary to identify differences in the DNA methylation status between HCCs and noncancerous livers to understand the contribution of epigenetic instability on the initiation and progression of HCC.

To clarify the genome-wide DNA methylation profiles in HCC, we used an Infinium HumanMethylation450 BeadChip array that can analyze >485,000 CpG sites distributed throughout the genome using a large number of human HCCs and noncancerous livers [10]. In addition, alterations in DNA methylation at each stage of tumor progression were also analyzed. We describe the unique distribution of CpG sites that had altered DNA methylation in HCC tissues, and describe the stepwise accumulation of abnormal DNA methylation during human hepatocarcinogenesis.

Materials and Methods

Patients

HCCs from 59 patients and 58 paired, noncancerous liver tissues were analyzed in this study. The tumors and paired noncancerous liver tissues were frozen immediately after surgical removal and stored at –80°C until DNA extraction. The clinical profiles of the patients are as follows: median age (25th–75th percentiles) was 65 years (59–72), 43 patients were male and 16 were female, 15 patients were positive for hepatitis B surface antigen (HBV positive), 23 were positive for hepatitis C virus (HCV) antibody (HCV positive), and 21 were negative for both HBV and HCV (virus negative). Four patients had liver fibrosis stage F0–F1, 7 had F2, 10 had F3, and 38 had F4. The median tumor size (25th–75th percentiles) was 3.0 cm (2.0–4.5). Written informed consent was obtained from all patients, and necessary approvals were obtained from the institutional review boards of the institution involved.

DNA Extraction/Bisulfite Treatment

Genomic DNA was extracted from frozen tissues using QIAamp DNA Mini Kits (Qiagen, Inc., Valencia, Calif., USA). Details of DNA extraction were described previously. After confirming DNA quality and concentration, 1 μg of genomic DNA was subjected to bisulfite treatment using the EZ DNA Methylation Kit (Zymo Research Corporation, Irvine, Calif., USA).

Methylation Analysis Using HumanMethylation450 BeadChip

Genome-wide DNA methylation profiles were assayed using a HumanMethylation450 BeadChip (Illumina, San Diego, Calif., USA) that contains probes covering >485,000 loci [10]. Whole genome amplification of DNA, enzymatic fragmentation, isopropanol precipitation and resuspension were performed followed by hybridization onto the BeadChips for 23 h. After washing away the unhybridized and nonspecific DNA and incorporation of the fluorescence-labeled oligonucleotide, images were obtained using the Illumina iScan SQ scanner (iScan Control v.3.2.45 software) and intensities of the images were extracted using GenomeStudio (v.2011.1) and Methylation Module (v.1.9.0) software. The obtained data were normalized with the background subtracted and to internal controls.

The methylation level was computed as a β value according to the normalized probe fluorescence intensity ratios between methylated and unmethylated signals: β value = signal intensity of the methylated allele/(sum of signal intensity of the unmethylated and methylated allele + 100). To evaluate the fidelity of the obtained β value and remove noise, each β value was accompanied by a detection p value indicating signals significantly greater than background. Probes containing single nucleotide polymorphisms or accompanied by single nucleotide polymorphisms within 10 bp from the 3′ end of the probe, and the probes on sex chromosomes were eliminated from the analysis to avoid methylation bias due to single nucleotide polymorphism and gender differences [11].

Extraction of Differentially Methylated CpGs and Statistics

Extraction of differentially methylated CpGs (DM-CpGs) from HCCs and surrounding noncancerous livers was performed as follows. First, we selected the CpG sites that had methylation differences between HCCs and noncancerous livers with a mean difference in the β value ≥0.15. Then, the Mann-Whitney U test and the false discovery rate control (Benjamini-Hochberg procedure) were applied for multiple comparisons. For the characterization of the DM-CpGs, we selected the 38,330 CpG sites showing a corrected value of $p < 1.0 \times 10^{-13}$. The Mann-Whitney U test was also performed to identify differences in the distribution between DM-CpGs and all CpGs on the BeadChip. For this purpose, the percentage of CpGs located within 1,500 bps of a transcription start site (TSS1500), 200 bp of a transcription start site (TSS200), 1st exon, 5′ untranslated region (UTR), body and 3′UTR were determined to identify differences in the distribution of CpGs in relation to gene structures. Similarly, to determine differences in the distribution in relation to CpG islands, the percentages of CpGs within a CpG island, CpG island shore (up to 2 kb away from islands), CpG island shelf (2–4 kb away from islands) and open sea (regions with isolated CpGs in the genome) were calculated. For the classification of tissues based on their methylation profile, we applied hierarchical clustering analysis using the β value of the top 1,000 DM-CpGs showing large methylation differences between HCCs and noncancerous livers. A principal component analysis (PCA) was also applied using the β value of these top 1,000 DM-CpGs. The χ^2 test was employed for comparisons of categorical variables. Student's t test was used for comparisons of two continuous variables.

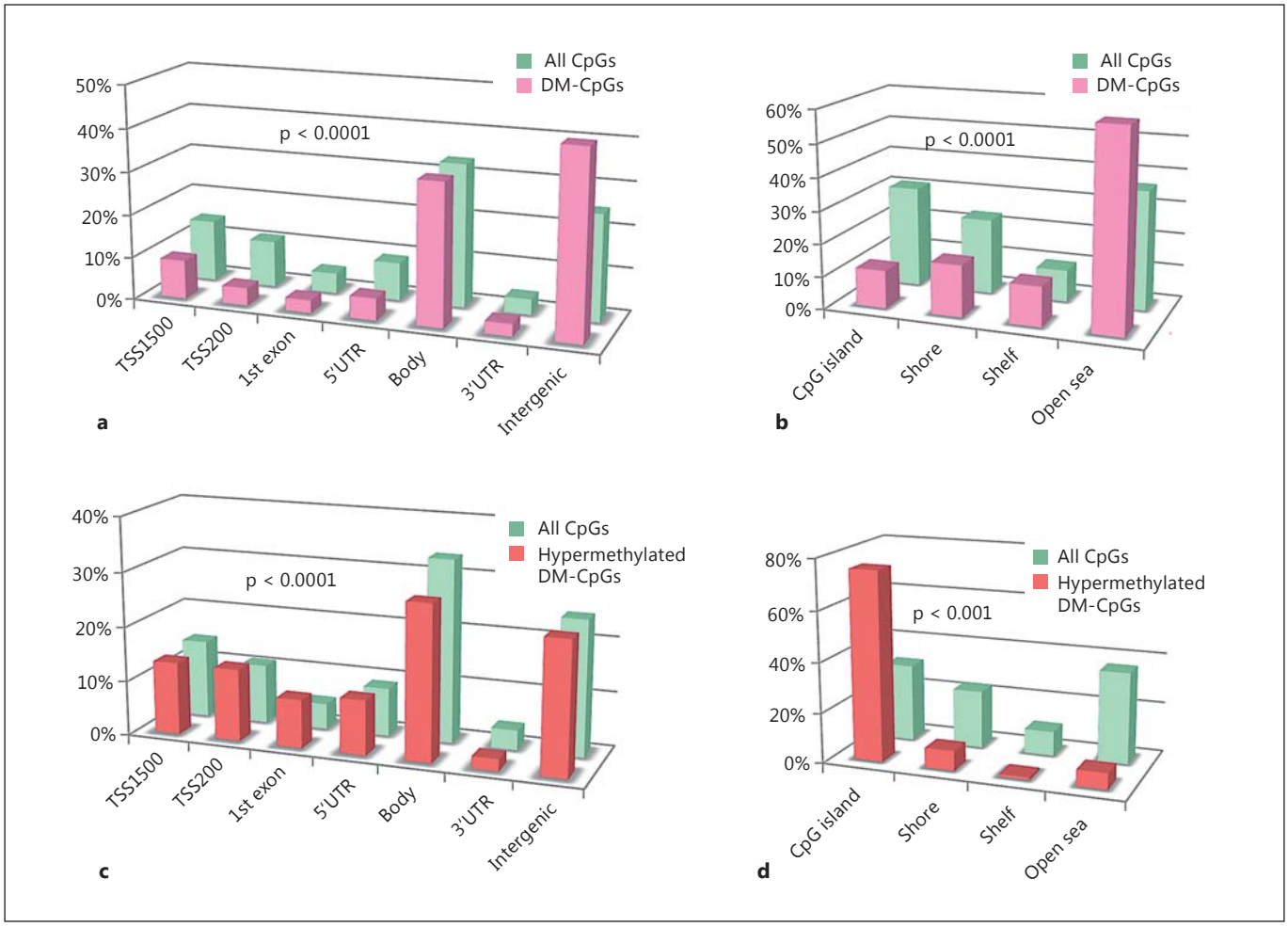

Color version available online

Fig. 1. Differences in the distribution of DM-CpGs and all CpGs on BeadChip arrays. DM-CpG and overall CpG distribution in relation to gene structure (**a**) and CpG islands (**b**). Hypermethylated DM-CpG and overall CpG distribution in relation to gene structure (**c**) and CpG islands (**d**). The bars indicate the distribution of DM-CpGs and all CpGs on the BeadChip (**a**, **b**) and the distribution of hypermethylated DM-CpGs and all CpGs (**c**, **d**). The y-axis shows the percentage of CpGs within each region among the CpGs analyzed. The p value was calculated using the Mann-Whitney U test for all comparisons. DM-CpGs were predominantly distributed within the intergenic regions (**a**) and open sea (**b**). On the other hand, hypermethylated DM-CpGs were distributed preferentially near the transcription start site (**c**) and within CpG islands (**d**).

All p values were two sided, and $p < 0.05$ was considered to be statistically significant. All statistical analyses were conducted using the R language (www.r-project.org) and JMP version 9.0 software (SAS Institute Inc., Cary, N.C., USA).

Results

Characteristics of DM-CpGs between HCCs and Noncancerous Livers

To determine differences in the methylation status between HCCs and noncancerous livers, we analyzed the distribution of 38,330 DM-CpGs. Among the 38,330 DM-CpGs, 35,279 (92%) showed decreased methylation in HCC tissues compared to the noncancerous liver tissues (hypomethylated DM-CpGs). Increased methylation in HCCs was observed at only 3,051 DM-CpGs (hypermethylated DM-CpGs: 8%). However, the absolute difference in the β value between HCCs and noncancerous livers was significantly larger at the hypermethylated DM-CpGs than the hypomethylated DM-CpGs (mean difference and 95% confidence interval, CI, were 0.285 and 0.283–0.287 for hypermethylated DM-CpGs, and 0.266 and 0.266–0.267 for hypomethylated DM-CpGs, respectively; $p < 0.0001$, Student's t test).

Figure 1a shows the distribution of the 38,330 DM-CpGs compared to all CpGs on the BeadChip. DM-CpGs occur more often in intergenic regions compared to all CpGs (16,507/38,330; 43% for DM-CpGs and 119,717/485,577; 24.7% for all CpGs). On the other hand, the proportion of DM-CpGs within the regions near the transcription start site is smaller than that for all CpGs (9.0, 4.0, 3.0 and 5.1% within TSS1500, TSS200, 1st exon and 5′UTR for DM-CpGs, and 14.2, 10.8, 4.7 and 8.8% within TSS1500, TSS200, 1st exon and 5′UTR for all CpGs, respectively). The difference in distributions between DM-CpGs and all CpGs on the BeadChip array was statistically significant ($p < 0.0001$, Mann-Whitney U test). Similarly, DM-CpGs were more often observed within open sea compared to all CpGs ($p < 0.0001$, Mann-Whitney U test; fig. 1b). When only the 3,051 hypermethylated DM-CpGs were considered, they were more often observed within regions near the transcription start site (13.3, 13.2, 8.8 and 10.0% within TSS1500, TSS200, 1st exon and 5′UTR, respectively) compared to all CpGs (14.2, 10.8, 4.7 and 8.8% within TSS1500, TSS200, 1st exon and 5′UTR, respectively; $p < 0.0001$, Mann-Whitney U test; fig. 1c). The distribution of hypermethylated DM-CpGs was also prominent within CpG islands and rare within open sea compared to all CpGs (75.2% within CpG islands and 6.5% within open sea for hypermethylated DM-CpGs vs. 30.9% within CpG islands and 36.3% within open sea for all CpGs; $p < 0.0001$, Mann-Whitney U test; fig. 1d).

Methylation Profile of DM-CpGs and Progression of HCC

We also determined the background factors of HCC that were associated with the methylation profile of the tumors. For this purpose, we selected the top 1,000 DM-CpGs showing large methylation differences between HCC and noncancerous liver tissues, and conducted a hierarchical clustering analysis using the β value of the top 1,000 DM-CpGs (fig. 2a). We examined the following clinical factors for this association: age (≥70 vs. <70 years), sex, etiology (HBV positive vs. HCV positive vs. virus negative), F-stage (F0–2 vs. F3–4), differentiation (well vs. moderately and poorly) and tumor size (>2.0 vs. ≤2.0 cm). Among them, tumor size had a significant association with the methylation profile of the selected 1,000 DM-CpGs, with tumors ≤2.0 cm associated with higher methylation levels ($p = 0.0028$, χ^2 test). Although not statistically significant, etiology classified by the presence of hepatitis virus also showed an association with the methylation-based classification ($p = 0.0540$, χ^2 test; data not shown). Therefore, we separated the HBV-positive, HCV-positive and virus-negative HCCs, and conducted PCA for each group using the β value of the top 1,000 DM-CpGs. Among the HCV-positive tumors, the first three principal components seemed to distinguish tumors ≤2.0 cm in size, which were distributed closer to noncancerous liver tissues, from tumors >2.0 cm. Figure 2b shows the 3D scatter diagram of PCA for HCV-positive liver tissues. However, the principal components failed to distinguish the tumors by their size in HBV-positive and virus-negative cases (data not shown). We further classified the HCV-positive liver tissues using a hierarchical clustering analysis (fig. 2c). HCV-positive liver tissues were clearly classified into two clusters with all HCCs in one cluster (cluster A) and all noncancerous liver tissue in the other cluster (cluster B). The HCC cluster could be further subdivided into A1 and A2. Interestingly, 4 of 5 HCCs (80.0%) in cluster A2 had a tumor size ≤2.0 cm. In contrast, only 3 of 18 HCCs (16.7%) in cluster A1 had a tumor size ≤2.0 cm. The association between methylation profile and tumor size was statistically significant for HCV-positive cases ($p = 0.0001$, χ^2 test; fig. 2d**)**.

Discussion

It is well known that carcinogenesis is a multistep process involving mutation and subsequent clonal expansion of the mutated cells, and the accumulation of genetic and epigenetic alterations are hallmarks of the cancer genome, including HCC [3, 6]. In this study, we tried to clarify alterations in DNA methylation in HCC, one of the characteristics of epigenetic alterations, using the HumanMethylation450 BeadChip array. We clarified the characteristics of CpGs that showed differences in methylation levels between HCC and noncancerous liver tissues using a large number of samples. We also identified stepwise progression of DNA methylation changes during the development of HCC, especially in HCV-related hepatocarcinogenesis.

In this study, we comprehensively characterized CpGs that were differentially methylated between HCC and noncancerous liver tissues of HCC patients. As reported previously, >90% of DM-CpGs showed hypomethylation in cancer [12]. Our analyses also identified that the DM-CpGs were predominantly located within intergenic regions. In addition, DM-CpGs in the genome were prominent within the open sea, the region showing isolated CpGs. From this point of view, DNA hypomethylation in

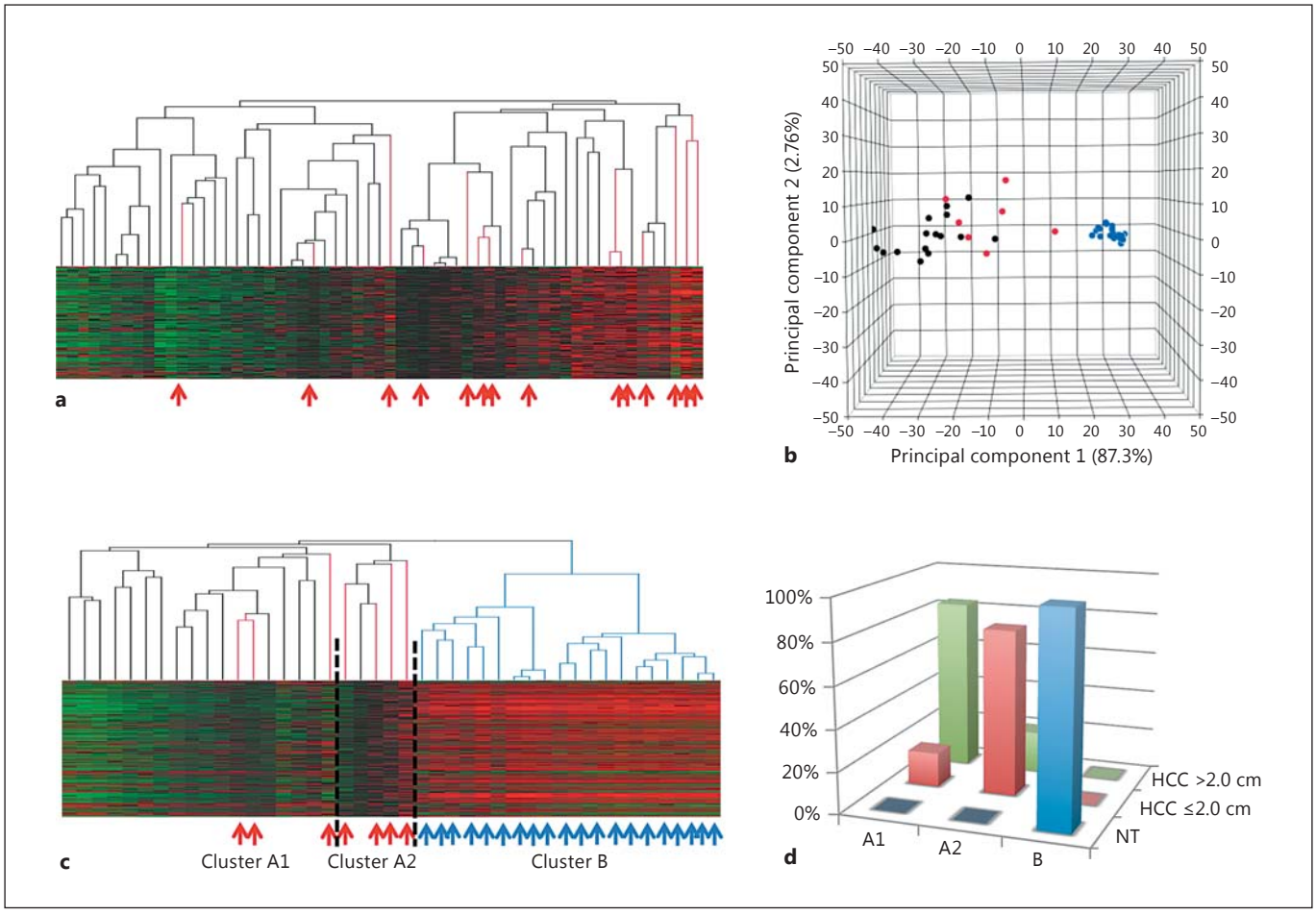

Color version available online

Fig. 2. Methylation profiles of noncancerous livers and HCCs classified by tumor size (colors are available in the only version only). **a**. Hierarchical clustering analysis of HCCs using the β value of the top 1,000 DM-CpGs. Tumors ≤2.0 cm were more frequent in the groups with higher methylation levels ($p = 0.0028$, χ^2 test). Heat map: green = decreased methylation density; red = increased methylation density; black = unchanged. Red arrows show HCCs ≤2.0 cm. **b** 3D scatter diagram of PCA for HCV-positive liver tissues using the β value of the top 1,000 DM-CpGs. Blue dots represent noncancerous livers, red dots HCCs ≤2.0 cm and black dots HCCs >2.0 cm. **c** Hierarchical clustering analysis for HCV-positive liver tissues. The clusters are divided into A1, A2 and B. Blue arrows show noncancerous livers and red arrows HCCs ≤2.0 cm. The samples without an arrow denote HCCs >2.0 cm. **d** Association between classifications based upon methylation profile and tumor size in HCV-positive liver tissues. A1, A2 and B correspond to the classification shown in **c**. Blue bars denote the distribution of noncancerous liver tissue (NT), red bars HCCs ≤2.0 cm and green bars HCCs >2.0 cm. $p < 0.0001$ (χ^2 test).

HCC might contribute to hepatocarcinogenesis through the activation of transcription in non-protein-coding regions, such as noncoding RNA and transposable elements [13]. We also found that global hypomethylation in HCC was associated with chromosomal instability [14], suggesting that the DNA hypomethylation could induce chromosomal fragility and play a role in human hepatocarcinogenesis. In contrast, hypermethylated DM-CpGs were mainly located within the region from TSS200 to the 1st exon, in close proximity to the gene promoter, and were predominantly observed within CpG islands. As the promoters within CpG islands generally regulate gene transcription by DNA methylation [9, 15], it is possible that hypermethylation of DNA could be responsible for HCC emergence mainly through the transcriptional inactivation of tumor suppressor genes.

DM-CpGs clearly discriminated HCCs from noncancerous livers by PCA and hierarchical clustering analysis. Interestingly, in HCC tissues, PCA and hierarchical clustering analysis using β values of DM-CpGs classified

HCCs into two subgroups according to tumor size (≤2.0 vs. >2.0 cm). The methylation profiles of smaller tumors were relatively similar to those of noncancerous livers compared to the methylation profiles of larger tumors. Therefore, stepwise progression of methylation alterations may take place during the development of HCC. Many studies have reported that DNA hypomethylation in tumors is associated with aggressive tumors showing rapid growth [16, 17]. We previously reported that the number of genes with hypermethylation increased with tumor progression [18]. From this point of view, accumulation of epigenetic alterations could be important for the progression of HCC, especially in HCV-positive cases [19]. However, we could not detect an association between methylation progression and tumor size in HBV-positive and virus-negative tumors. Further analyses using a large number of HCCs should clarify the accumulation of methylation events in HBV-positive and virus-negative hepatocarcinogenesis.

In this study, we clarified the characteristic feature of CpGs that had differences in methylation levels between HCCs and noncancerous livers. Furthermore, progressive alterations in DNA methylation were observed in HCV-related hepatocarcinogenesis. The comprehensive data on DNA methylation obtained here should be of importance to better understand the molecular mechanisms of multistep progression of epigenetic alterations during human hepatocarcinogenesis.

References

1 Kim do Y, Han KH: Epidemiology and surveillance of hepatocellular carcinoma. Liver Cancer 2012;1:2–14.
2 Kudo M: Prediction of hepatocellular carcinoma incidence risk by ultrasound elastography. Liver Cancer 2014;3:1–5.
3 Nishida N, Goel A: Genetic and epigenetic signatures in human hepatocellular carcinoma: a systematic review. Curr Genomics 2011; 12:130–137.
4 Moeini A, Cornella H, Villanueva A: Emerging signaling pathways in hepatocellular carcinoma. Liver Cancer 2012;1:83–93.
5 Ramakrishna G, Rastogi A, Trehanpati N, Sen B, Khosla R, Sarin SK: From cirrhosis to hepatocellular carcinoma: new molecular insights on inflammation and cellular senescence. Liver Cancer 2013;2:367–383.
6 Nishida N: Alteration of epigenetic profile in human hepatocellular carcinoma and its clinical implications. Liver Cancer, in press.
7 Esteller M: Epigenetics in cancer. N Engl J Med 2008;358:1148–1159.
8 Berdasco M, Esteller M: Aberrant epigenetic landscape in cancer: how cellular identity goes awry. Dev Cell 2010;19:698–711.
9 Herman JG, Baylin SB: Gene silencing in cancer in association with promoter hypermethylation. N Engl J Med 2003;349:2042–2054.
10 Marabita F, Almgren M, Lindholm ME, Ruhrmann S, Fagerstrom-Billai F, Jagodic M, Sundberg CJ, Ekstrom TJ, Teschendorff AE, Tegner J, Gomez-Cabrero D: An evaluation of analysis pipelines for DNA methylation profiling using the Illumina HumanMethylation450 BeadChip platform. Epigenetics 2013;8:333–346.
11 Shen J, Wang S, Zhang YJ, Wu HC, Kibriya MG, Jasmine F, Ahsan H, Wu DP, Siegel AB, Remotti H, Santella RM: Exploring genome-wide DNA methylation profiles altered in hepatocellular carcinoma using Infinium HumanMethylation 450 BeadChips. Epigenetics 2013;8:34–43.
12 Song MA, Tiirikainen M, Kwee S, Okimoto G, Yu H, Wong LL: Elucidating the landscape of aberrant DNA methylation in hepatocellular carcinoma. PLoS One 2013;8:e55761.
13 Kulis M, Queiros AC, Beekman R, Martin-Subero JI: Intragenic DNA methylation in transcriptional regulation, normal differentiation and cancer. Biochim Biophys Acta 2013; 1829:1161–1174.
14 Nishida N, Kudo M, Nishimura T, Arizumi T, Takita M, Kitai S, Yada N, Hagiwara S, Inoue T, Minami Y, Ueshima K, Sakurai T, Yokomichi N, Nagasaka T, Goel A: Unique association between global DNA hypomethylation and chromosomal alterations in human hepatocellular carcinoma. PLoS One 2013; 8:e72312.
15 Nishida N, Kudo M: Oxidative stress and epigenetic instability in human hepatocarcinogenesis. Dig Dis 2013;31:447–453.
16 Mudbhary R, Hoshida Y, Chernyavskaya Y, Jacob V, Villanueva A, Fiel MI, Chen X, Kojima K, Thung S, Bronson RT, Lachenmayer A, Revill K, Alsinet C, Sachidanandam R, Desai A, SenBanerjee S, Ukomadu C, Llovet JM, Sadler KC: UHRF1 overexpression drives DNA hypomethylation and hepatocellular carcinoma. Cancer Cell 2014;25:196–209.
17 Gao XD, Qu JH, Chang XJ, Lu YY, Bai WL, Wang H, Xu ZX, An LJ, Wang CP, Zeng Z, Yang YP: Hypomethylation of long interspersed nuclear element-1 promoter is associated with poor outcomes for curative resected hepatocellular carcinoma. Liver Int 2014;34: 136–146.
18 Nishida N, Kudo M, Nagasaka T, Ikai I, Goel A: Characteristic patterns of altered DNA methylation predict emergence of human hepatocellular carcinoma. Hepatology 2012;56: 994–1003.
19 Nishida N, Nagasaka T, Nishimura T, Ikai I, Boland CR, Goel A: Aberrant methylation of multiple tumor suppressor genes in aging liver, chronic hepatitis, and hepatocellular carcinoma. Hepatology 2008;47:908–918.